

Search for physics beyond the standard model in events with leptons and jets at CMS

James F. Hirschauer*

On behalf of the CMS Collaboration

Fermi National Accelerator Laboratory

E-mail: james.francis.hirschauer@cern.ch

Many theories of new physics predict the existence of new particles decaying to leptons and hadronic jets, including leptoquarks of grand unified theories, heavy neutrinos and right-handed W_R bosons of left-right symmetric extensions of the standard model, heavy Majorana neutrinos that mix with the standard model lepton sector, and scalar quarks in supersymmetric theories that violate R -parity. The results of searches for these particles, in final states including jets, electrons, muons, and tau leptons, are reported. The studies are based on samples of proton-proton collisions at $\sqrt{s} = 7$ TeV (corresponding to 5.0 fb^{-1} and 4.8 fb^{-1} of integrated luminosity) and $\sqrt{s} = 8$ TeV (corresponding to 3.6 fb^{-1} of integrated luminosity) collected with the CMS detector at the CERN Large Hadron Collider. Based on good agreement of the data with the standard model expectations, the data are used to determine limits on new particle production at the 95% confidence level.

*36th International Conference on High Energy Physics,
July 4-11, 2012
Melbourne, Australia*

*Speaker.

1. Introduction

We describe searches for several new particles: first- (LQ1) and second-generation (LQ2) scalar leptoquarks [1], third-generation scalar (LQ3) and vector leptoquarks (VLQ) [2], the scalar partner of the top quark (stop) from supersymmetry (SUSY) models with R -parity violation (RPV) [2], heavy neutrinos (either Dirac or Majorana) and right-handed W_R bosons of left-right symmetric extensions (LRSM) of the standard model (SM) [3], and heavy Majorana neutrinos [4]. The searches are performed in events with two quarks and two leptons of the same flavor; the leptons are either both charged or one charged and one neutral. Since the quarks manifest as hadronic jets (j) and the neutral leptons as missing transverse energy (E_T^{miss}), we search in final states of $eejj$, $\mu\mu jj$, $\tau\tau jj$, $ejj + E_T^{\text{miss}}$, and $\mu jj + E_T^{\text{miss}}$. In final states with τ , we require that the jets are identified as originating from b -quark hadronization (b-tagged jets, or b jets). The studies are based on samples of pp collisions at $\sqrt{s} = 7$ TeV (corresponding to 5.0 fb^{-1} and 4.8 fb^{-1} of integrated luminosity) and $\sqrt{s} = 8$ TeV (corresponding to 3.6 fb^{-1} of integrated luminosity) recorded with the CMS detector [5] at the CERN Large Hadron Collider (LHC).

These proceedings are intended as a brief reference for readers seeking to qualitatively understand the motivations, experimental methods, and tested theories of the studies described herein. We refer the reader to the individual papers [1, 2, 3, 4] for many of the details of each analysis, including relevant references.

2. Basic Reconstruction and Selection

Electron candidates are reconstructed from energy clusters in the electromagnetic calorimeter that have a shower shape consistent with that of an electron, that are matched to hits in the central tracker, and that are isolated from other energy deposits in the calorimeter and reconstructed tracks. Muons are reconstructed from pairs of matched tracks from the muon and tracking systems and are also required to be isolated. Jets, hadronically decaying τ leptons, and E_T^{miss} are reconstructed with a particle-flow algorithm, which identifies and measures stable particles by combining information from all CMS sub-detectors. We identify b jets using a displaced track counting algorithm based on track impact parameter significance. These candidates have transverse momentum p_T exceeding 30-40 GeV, pseudorapidity η less than 2.1-2.5, and spatial separation $\sqrt{(\Delta\phi)^2 + (\Delta\eta)^2}$ greater than 0.5-0.8, depending on particle type and analysis.

In all studies, the data are observed to agree with the SM expectation, which is estimated from both Monte Carlo (MC) simulations and data control samples. Limits are computed at the 95% confidence level (CL) with the modified frequentist CL_s method based on profile likelihood ratio test statistics constructed from the Poisson probability for the observed number of events given the expectations for background and signal. In some cases, correlated and uncorrelated observations from separate datasets or event categories are statistically combined via the likelihood.

3. Searches for Leptoquarks and Scalar Tops

As part of the explanation of the underlying relationship between quarks and leptons, many extensions of the SM, including grand unified theories, composite models, and superstring-inspired

models, predict the existence of particles that couple to both quarks and leptons. These leptoquarks (LQ) have spin zero or one and decay to a charged lepton and a quark with an unknown branching fraction β or to a neutrino and a quark with branching fraction $1 - \beta$. To satisfy constraints from bounds on flavor-changing neutral currents and from rare pion and kaon decays, LQ are assumed to couple only to quarks and leptons of a single SM generation. Depending on the generation to which they couple, LQ are classified as first-, second-, or third-generation. At the LHC, LQ would be produced in pairs via gluon-gluon fusion and quark-antiquark annihilation.

3.1 Search for first- and second-generation leptoquarks

We search for LQ1 (LQ2) in the $eejj$ and $evjj$ ($\mu\mu jj$ and $\mu\nu jj$) final states in a sample of pp collisions at $\sqrt{s} = 7$ TeV corresponding to 5.0 fb^{-1} of integrated luminosity. For the $eejj$ analysis, events are required to pass a double-electron trigger or a double-photon trigger with a 33 GeV p_T threshold. For the $evjj$ analysis, events pass either a single-electron trigger or a trigger requiring an electron with $p_T > 17\text{-}30$ GeV, $E_T^{\text{miss}} > 15\text{-}20$ GeV, and two jets with $p_T > 25\text{-}30$ GeV; the thresholds vary according to the instantaneous luminosity to keep trigger rates approximately constant. For the LQ2 analyses, events are required to pass a single-muon trigger with a p_T threshold of 40 GeV.

The sensitivities of the $\ell\ell jj$ searches are optimized with thresholds on the dilepton invariant mass ($M_{\ell\ell}$), the scalar sum of the p_T of leptons and jets (S_T), and the smaller of the lepton-jet invariant masses from the pairing that minimizes the LQ- \bar{LQ} invariant mass difference ($M_{\ell j}^{\text{min}}$). In the $\ell\nu jj$ search, we require that the lepton- E_T^{miss} transverse mass M_T exceed 120 GeV, and the sensitivity is then optimized with requirements on E_T^{miss} , S_T , and $M_{\ell j}$, which is defined as the lepton-jet invariant mass from the pairing that minimizes the LQ- \bar{LQ} transverse mass difference. Depending on LQ mass hypothesis and final state, the thresholds are 100-150 GeV for $M_{\ell\ell}$, 330-1000 GeV for S_T , 60-520 GeV for $M_{\ell j}^{\text{min}}$, 100-240 GeV for E_T^{miss} , and 150-540 GeV for $M_{\ell j}$.

The main SM backgrounds in the $\ell\ell jj$ channel are $Z/\gamma^* + \text{jets}$ and $t\bar{t}$ events. We obtain the $Z/\gamma^* + \text{jets}$ background prediction from MC that has been normalized with data for which $M_{\ell\ell}$ is consistent with that of a Z boson. The $t\bar{t}$ contribution is estimated from an $e\mu$ data sample with appropriate corrections for differences in electron and muon efficiency and assuming ee and $\mu\mu$ rates are half the $e\mu$ rate. The main SM backgrounds in the $\ell\nu jj$ channels are $W + \text{jets}$ and $t\bar{t}$, which are estimated from MC that has been normalized using data with low M_T .

The dominant sources of systematic uncertainty on the expected signal are the jet energy scale (2-3%), muon reconstruction efficiency (2%), and the integrated luminosity (2.2%). The dominant uncertainty on the background expectation comes from the extrapolation from $Z/\gamma^* + \text{jets}$ and $W + \text{jets}$ control samples (11%).

In Fig. 1, we show the 95% exclusion regions as a function of β and LQ1 mass and LQ2 mass from the statistical combinations of $\ell\ell jj$ and $\ell\nu jj$ channels. The limits on LQ masses are shown in Table 1.

3.2 Search for third-generation leptoquarks and scalar quarks

We search for LQ3, VLQ, and stops decaying into a τ and b quark in a sample of pp collisions at $\sqrt{s} = 7$ TeV corresponding to 4.8 fb^{-1} of integrated luminosity. In SUSY, a large mixing angle

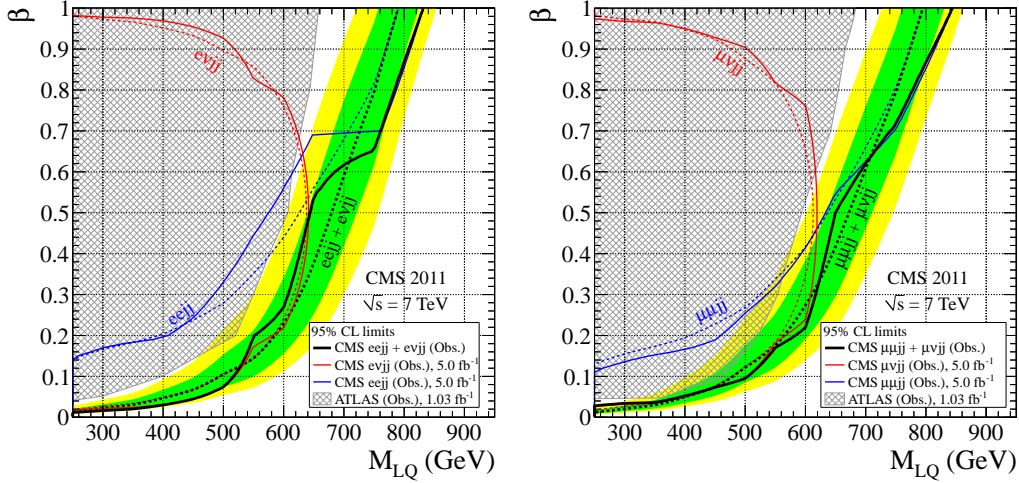


Figure 1: Left (Right) frame: the expected and observed exclusion limits at 95% CL on the LQ1 (LQ2) hypothesis in the β versus mass plane using the central value of signal cross section for the individual $eejj$ and $evjj$ ($\mu\mu jj$ and $\mu\nu jj$) channels and their combination. The dark green and light yellow expected limit uncertainty bands represent the 68% and 95% confidence intervals. Solid lines represent the observed limits in each channel, and dashed lines represent the expected limits. The shaded region is excluded by the current ATLAS limits [6, 7].

between the left-chiral (\tilde{t}_L) and right-chiral (\tilde{t}_R) stops can produce two mass eigenstates, \tilde{t}_1 and \tilde{t}_2 , with a large mass splitting and $M_{\tilde{t}_1}$ substantially smaller than the masses of the other scalar SUSY particles. Additionally, in RPV SUSY models, trilinear RPV operators allow the lepton-number-violating decay $\tilde{t}_L \rightarrow \tau b$ with a coupling λ'_{333} . Assuming λ'_{333} and $\tilde{t}_L \rightarrow \tau b$ branching fraction ($B_{\tau b}^{\tilde{t}_L}$) to be unity, stop and LQ3 production and decay are identical, and the search results are applicable to both particles. In addition to this simple interpretation, we also consider an MSSM-based benchmark scenario in which $B_{\tau b}^{\tilde{t}_L}$ decreases with increasing stop mass as R -parity-conserving decays become kinematically accessible; the MSSM parameters used in this scenario are in Ref. [2]. We consider a range of λ'_{333} from 1 to $\mathcal{O}(10^{-7})$, below which the decay length exceeds 0.5 mm making this analysis insensitive because of vertex requirements.

In addition to requiring b-tagged jets, we require that one τ in each event decays leptonically and the other hadronically (τ_h) yielding final states of $\tau_h \mu bb$ and $\tau_h ebb$. Events are required to pass τ_h +electron or τ_h +muon triggers with lepton p_T thresholds of 15-20 GeV and 12-20 GeV, respectively, depending on the data-taking period. We require that the τ_h -b invariant mass $M_{\tau_h b}$ exceed 170 GeV; $M_{\tau_h b}$ is defined with the particle pairing that minimizes the LQ- $\bar{L}Q$ invariant mass difference. The observed and expected event counts are examined as functions of the $\tau_h \ell bb$ S_T . The primary SM backgrounds are $t\bar{t}$, Z+jets, and W+jets events. The $t\bar{t}$ background is estimated from simulation that has been normalized with the low- $M_{\tau_h b}$ data sample. The Z+jets and W+jets backgrounds, in which one jet is misidentified as τ_h , are estimated from the data. The dominant sources of systematic uncertainty on the expected signal are the jet energy scale (2-4%) and the integrated luminosity (2.2%). The dominant uncertainty on the background expectation comes from the normalization of the $t\bar{t}$ MC (13-17%) and the estimation of Z+jets and W+jets backgrounds (40%).

In Fig. 2, we show 95% CL limits on the effective cross section as a function of particle mass, and the 95% CL exclusion region as a function of λ'_{333} and stop mass for two values of the heavy SU(2) gaugino mass M_2 . By comparing predicted cross sections to the limit, we obtain limits on particle mass, which are show in Table 1.

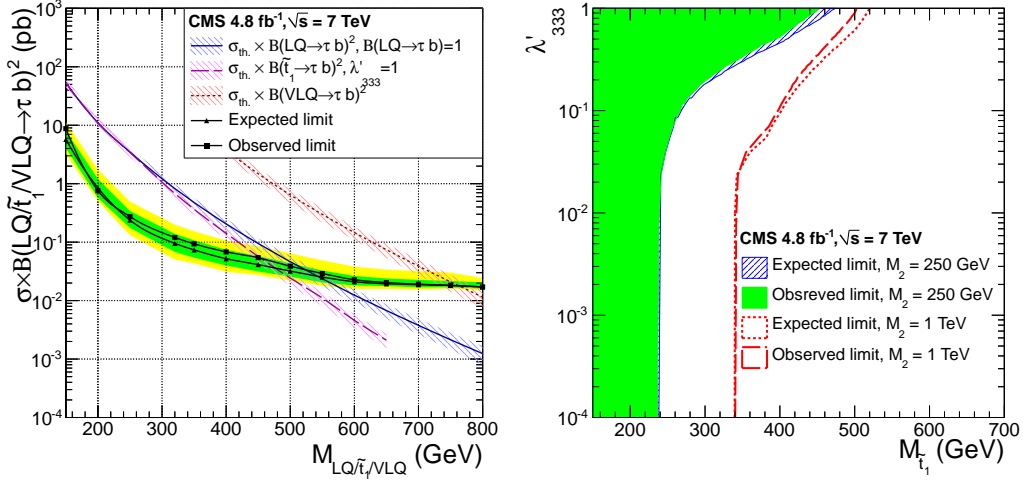


Figure 2: Left: the expected and observed upper limit at 95% CL on the product of cross section and τb branching fraction as a function of mass. The $\pm 1\sigma$ and $\pm 2\sigma$ uncertainties on the expected limit are also shown as green (inner) and yellow (outer) bands about the expected limit. The blue (solid) curve, magenta (dashed) curve, and red (dotted) curves and the matching shaded bands represent the theoretical LQ3, \tilde{t}_1 , and VLQ pair production cross sections with theoretical uncertainty. Right: limits at 95% CL on the RPV coupling λ'_{333} as a function of \tilde{t}_1 for $M_2 = 250$ GeV and $M_2 = 1$ TeV.

4. Search for the heavy neutrinos and W_R bosons in a left-right symmetric model

We search for production of heavy neutrinos (N_e, N_μ) and W_R bosons of the LRSM in samples of pp collisions at $\sqrt{s} = 7$ and $\sqrt{s} = 8$ TeV corresponding to 5.0 fb $^{-1}$ and 3.6 fb $^{-1}$ of integrated luminosity, respectively. The LRSM was initially proposed to explain parity violation in electroweak interactions as the result of a spontaneously broken left-right symmetry; additionally, the large mass of N_ℓ can explain the very small masses of SM neutrinos through the see-saw mechanism. The LRSM produces $\ell\ell jj$ ($\ell = e, \mu$) final states through the process $pp \rightarrow W_R \rightarrow \ell N_\ell$, with $N_\ell \rightarrow \ell W_R^*$, followed by $W_R^* \rightarrow jj$. We assume that left and right gauge couplings are the same and that $W_R - W_L$ and $N_\ell - N_{\ell'}$ mixing is small.

Events are collected with double electron and single muon triggers. We require that the leading lepton have $p_T > 60$ GeV and $M_{\ell\ell} > 200$ GeV, and we examine the four-object mass distribution with $M_{\ell\ell jj} > 600$ for evidence of W_R production. The primary backgrounds are $t\bar{t}$ and Z+jets, which are estimated as in the LQ searches. The dominant sources of systematic uncertainty on the expected signal are the lepton reconstruction efficiency (6-10%); the dominant uncertainty on the background expectation comes from shape uncertainties in $t\bar{t}$ and Z+jets MC (16-53%).

In Fig. 3, we show 3.6 fb $^{-1}$ of 8 TeV $eejj$ data compared to the background expectation and the 95% exclusion region as a function of W_R and N_ℓ masses (M_{W_R}, M_{N_ℓ}) from the statistical

combination of the results from the 7 TeV and 8 TeV $\mu\mu jj$ datasets. The limits on M_{W_R} assuming $M_{N_\ell} = \frac{1}{2}M_{W_R}$ are shown in Table 1.

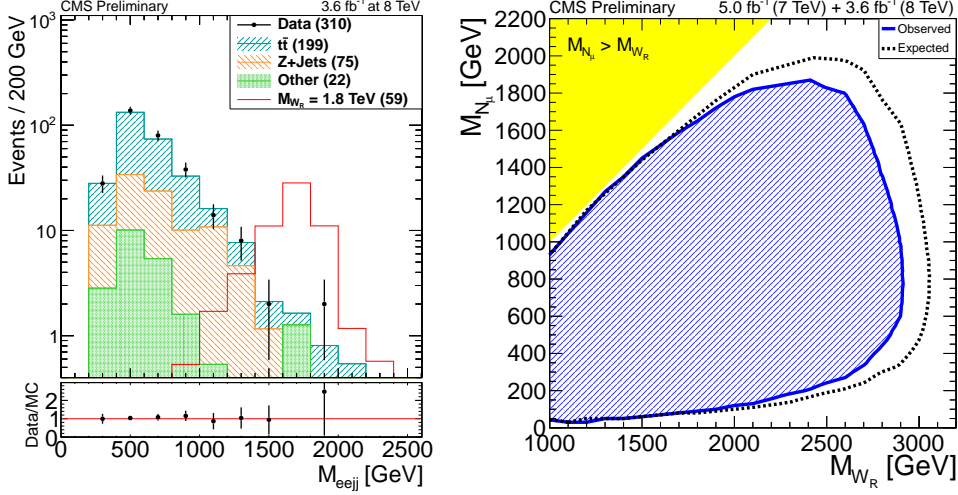


Figure 3: Left: Comparison of observed and expected $M_{\ell\ell jj}$ distributions in $eejj$ events passing all selection criteria except the M_{ee} requirement. Right: The 95% CL exclusion region as a function of M_{W_R} and M_{N_μ} from the combined 7 TeV and 8 TeV $\mu\mu jj$ datasets.

5. Search for the heavy Majorana neutrinos

We search for heavy Majorana neutrinos (N_ℓ^{Maj} , $\ell = e, \mu$) that couple to W bosons and leptons of the SM via the parameter $V_{\ell N}$ in a sample of pp collisions at $\sqrt{s} = 7$ TeV corresponding to 5.0 fb⁻¹ of integrated luminosity. The salient feature of the model is that the Majorana nature of N_ℓ^{Maj} allows lepton-number violation by two units and final states with leptons of the same charge and flavor ($\ell^\pm \ell^\pm jj$) via the process $pp \rightarrow W^\pm \rightarrow \ell^\pm N_\ell^{\text{Maj}}$, $N_\ell^{\text{Maj}} \rightarrow \ell^\pm W^\mp$, $W^\mp \rightarrow jj$. Because of the relatively small SM background, we require that the leptons have the same charge.

Events are collected with double lepton triggers with $p_T > 7-17$ GeV. After the requiring $E_T^{\text{miss}} < 50$ GeV, few events remain because of the same charge requirement. The primary backgrounds are QCD events with two misidentified isolated leptons and W+jets or $t\bar{t}$ events with one misidentified isolated lepton. These contributions are simultaneously estimated with data control samples. The dominant source of systematic uncertainty on the expected signal is the jet energy scale (3.3%); the dominant uncertainty on the background expectation comes from estimating the misidentification rate (35%).

In Fig. 4, we show the $eejj$ data compared to the background expectation and the 95% exclusion region as a function of N_ℓ^{Maj} mass (M_{N_ℓ}) and $|V_{\ell N}|^2$ in the $\mu\mu jj$ channel. The limits on M_{N_ℓ} for $|V_{\ell N}|^2 = 0.5$ are shown in Table 1. For $M_{N_\ell} = 90$ GeV the limits are $|V_{\mu N}|^2 < 0.07$ and $|V_{eN}|^2 < 0.22$. At $M_{N_\ell} = 210$ GeV the limits are $|V_{\mu N}|^2 < 0.43$, while for $|V_{eN}|^2$ the limit reaches 1.0 at a mass of 203 GeV. These are the first direct upper limits on $|V_{\ell N}|^2$ for $M_{N_\ell} > 90$ GeV.

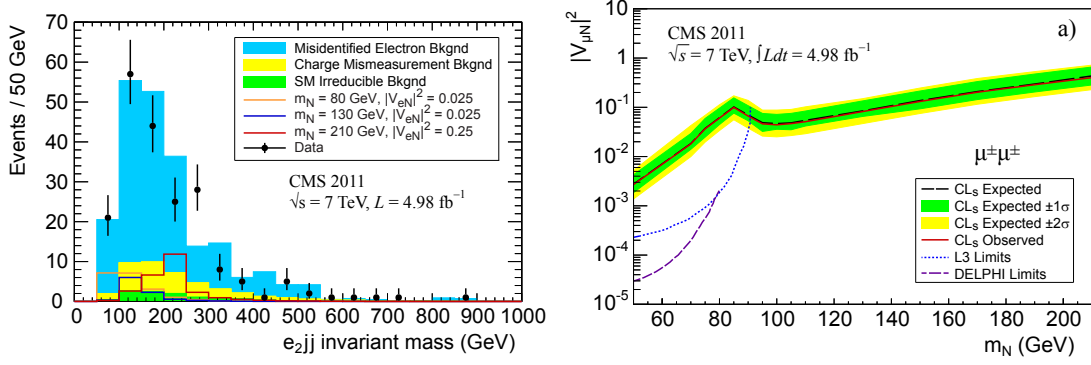


Figure 4: Left: Comparison of the observed and expected three object mass distributions in $eejj$ events. Right: The 95% CL exclusion region as a function of $|V_{\mu N}|^2$ and M_{N_μ} from the $\mu\mu jj$ dataset.

6. Summary

We describe searches for first-, second-, and third-generation scalar leptoquarks, third-generation vector leptoquarks, light stops in RPV SUSY, heavy neutrinos and W_R of the LRSM, and heavy Majorana neutrinos. The searches are performed in final states of $eejj$, $\mu\mu jj$, $eejj + E_T^{\text{miss}}$, $\mu jj + E_T^{\text{miss}}$, $\tau_h ebb$, and $\tau_h \mu bb$. The studies are based on samples of pp collisions at $\sqrt{s} = 7$ TeV (corresponding to 5.0 fb $^{-1}$ and 4.8 fb $^{-1}$ of integrated luminosity) and $\sqrt{s} = 8$ TeV (corresponding to 3.6 fb $^{-1}$ of integrated luminosity) recorded with the CMS detector in 2011 and 2012. The limits on masses of these particles, which are shown in Table 1, extend the previous limits as described in Refs. [1, 2, 3, 4].

Table 1: Summary of lower mass limits for LQ1, LQ2, LQ3, and VLQ for two values of β ; for stop from a simplified model with $B_{\tau b}^{\tilde{t}_1} = 1$ and from benchmark MSSM scenarios for two values of λ'_{333} ; and for W_R and the mass of a heavy Majorana neutrino for electron and muon final states. All entries have units of GeV.

Leptoquarks	$\beta = 0.5$	$\beta = 1.0$
LQ1	640	830
LQ2	650	840
LQ3	–	525
VLQ	–	760
Stops	$\lambda'_{333} = 1$	$\lambda'_{333} > \mathcal{O}(10^{-7})$
$\tilde{t}_1, B_{\tau b}^{\tilde{t}_1} = 1$	525	–
$\tilde{t}_1, M_2 = 250$ GeV	450	240
$\tilde{t}_1, M_2 = 1000$ GeV	–	340
Heavy Neutrinos	$eejj$	$\mu\mu jj$
$W_R, M_{N_i} = \frac{1}{2}M_{W_R}$	2500	2800
$N_i^{\text{Maj}}, V_{\ell N} ^2 = 0.5$	160	210

References

- [1] CMS Collaboration, arXiv:1207.5406 (2012); *Accepted by Phys. Rev. D.*
- [2] CMS Collaboration, arXiv:1210.5627 (2012); *Submitted to Phys. Rev. Lett.*
- [3] CMS Collaboration, CMS-PAS-EXO-12-017 (2012).
- [4] CMS Collaboration, Phys. Lett. B717 (2012) 109.
- [5] CMS Collaboration, JINST 3 (2008) S08004.
- [6] ATLAS Collaboration, Phys. Lett. B709 (2012) 158.
- [7] ATLAS Collaboration, arXiv:1112.4828 (2012); *Submitted to Eur. Phys. J. C.*